Projecting global urban land expansion and heat island intensification through 2050

Environmental Research Letters

LETTER

Projecting global urban land expansion and heat island intensification through 2050

Kangning Huang[1], Xia Li[2], Xiaoping Liu[3] and Karen C Seto[1]

[1] Yale School of Forestry and Environmental Studies, Yale University, New Haven, CT 06511, United States of America
[2] School of Geographic Sciences, Key Lab. of Geographic Information Science (Ministry of Education), East China Normal University, Shanghai 200241, People's Republic of China
[3] Guangdong Key Laboratory for Urbanization and Geo-simulation, School of Geography and Planning, Sun Yat-Sen University, Guangzhou 510275, People's Republic of China

E-mail: kangning.huang@yale.edu

Keywords: urbanization, urban climate, land change science, sustainability

Supplementary material for this article is available online

OPEN ACCESS

RECEIVED
15 May 2019

REVISED
2 September 2019

ACCEPTED FOR PUBLICATION
7 October 2019

PUBLISHED
14 November 2019

Abstract

Urban populations are expected to increase by 2–3 billion by 2050, but we have limited understanding of how future global urban expansion will affect urban heat island (UHI) and hence change the geographic distributions of extreme heat risks. Here we develop spatially explicit probabilistic global projections of UHI intensification due to urban land expansion through 2050. Our projections show that urban land areas are expected to expand by 0.6–1.3 million km^2 between 2015 and 2050, an increase of 78%–171% over the urban footprint in 2015. This urban land expansion will result in average summer daytime and nighttime warming in air temperature of 0.5 °C–0.7 °C, up to ~3 °C in some locations. This warming is on average about half, and sometimes up to two times, as strong as that caused by greenhouse gas (GHG) emissions (multi-model ensemble average projections in Representative Concentration Pathway 4.5). This extra urban expansion-induced warming, presented here, will increase extreme heat risks for about half of the future urban population, primarily in the tropical Global South, where existing forecasts already indicate stronger GHG emissions-warming and lack of adaptive capacity. In these vulnerable urban areas, policy interventions to restrict or redistribute urban expansion and planning strategies to mitigate UHIs are needed to reduce the wide ranges of impacts on human health, energy system, urban ecosystem, and infrastructures.

Introduction

By 2050, there will be an additional 2–3 billion people living in urban areas, where surface temperatures have been rising faster than the global mean (Stone 2012). Compared to rural areas, the stronger warming in urban areas is due to the local urban heat island (UHI) effect in addition to global climate change induced by greenhouse gas (GHG) emissions. Warming from GHG emissions is caused by retention of outgoing long-wave radiation while that from the UHI effect is mainly because of reduced evapotranspiration, increased solar radiation absorption, and anthropogenic waste heat (Oke 1982). Although urban areas are expected to expand over the next thirty years to accommodate the increase in the urban population (UN DESA 2014), the magnitude of this urban expansion is unknown. Moreover, despite previous local- and regional-scale studies and projections (Georgescu *et al* 2013, Stone *et al* 2014, Chen and Frauenfeld 2016, Merckx *et al* 2018), there is less scientific understanding of the aggregate effects of future urban expansion on the UHI effects globally. Without a global outlook of this extra urban expansion-warming on top of climate change, we may underestimate the actual warming that will be experienced by billions of urban dwellers and fail to identify which urban areas will be more vulnerable to extreme heat risks.

Here we develop spatially explicit, probabilistic projections of global urban land expansion and estimate their effects on UHI intensification and the

subsequent increase in global warming through 2050. The urban expansion projection model includes a novel mechanism to preserve the log-scale size distribution (Gabaix 1999) of urban clusters, the continuous unit of urban areas affected by spatially linked socioeconomic processes (Fragkias and Seto 2009). These projections assume the continuing trends of historical urban expansion and are based on the Shared Socioeconomic Pathways (SSP) scenarios used in the recent Intergovernmental Panel on Climate Change (IPCC) assessment report (O'Neill *et al* 2015). The forecasted future urban land areas are then used in a sigmoid-based empirical model to estimate the log-size dependent (Zhou *et al* 2013) UHI intensities with diurnal, seasonal, and intra-urban variations. The UHI models are divided among different Köppen–Geiger climate zones: arid, tropical, temperate, and cold climates (Kottek *et al* 2006). Finally, we overlay the population on urban land areas, UHI intensifications and GHG emissions-induced climate change to examine their relative impacts on exposure to heat risks in urban areas. By integrating these models and analyses, we aim to answer the following questions: Where and how much land will be converted to urban areas by mid-century? How will urban expansion affect UHI intensification across the world? What is the relative contribution of urban expansion-induced warming compared to that by GHG emissions? And, how will this warming reshape the geographic distributions of extreme heat risks?

Methods

Urban land expansion forecasts

By utilizing multi-year global urban land observation and preserving the Zipf's law of urban size distribution (Gabaix 1999, Fragkias and Seto 2009) in the forecasts, we significantly modify a global urban land change model, URBANMOD (Seto *et al* 2012, Güneralp and Seto 2013), to develop a new forecast model, called URBANMOD-ZIPF. To build this model, we use four sources of data: urban land extent from the Global Human Settlement Layer (Pesaresi *et al* 2013), urban population from the United Nations (UN DESA 2014), GDP from the World Bank (World Bank Group 2019), and future scenarios of the SSP from the International Institute for Applied Systems Analysis (Riahi et al 2017). This model has two phases: (1) predicting the quantities of urban land by 2050, and (2) allocating them spatially at 5 km resolution. In the first phase, we first use a fixed effect panel regression model to relate urban land per capita (ULC) to GDP per capita (GDPC), and then apply this model to forecast the amount of urban land for each region in each scenario. In the second phase, a land change model allocates these new urban lands using slope, distance to road, population density, and land cover as the drivers of land change. During the allocation process, the urban size distribution is preserved by adjusting the expansion magnitude of an urban cluster proportional to its size (Gabaix 1999). Although there is ongoing research on potentially more complex mechanisms to preserve Zipf's law (Rozenfeld *et al* 2008, Cristelli *et al* 2012), introducing a size-distribution-preserving mechanism, albeit a simple one, into urban land change modeling can improve the forecasts over the existing ones (Seto *et al* 2012, Güneralp and Seto 2013). While this mechanism can improve projections of most urban clusters, it may fail to capture the process that some individual cities move up in ranks: for instance, Los Angeles grew rapidly and replaced Chicago in 1980s to become the 2nd largest city in the United States.

In addition to extending the forecasting period of (Seto *et al* 2012) from 2030 to 2050, the new forecasts make two contributions to our understanding of urbanization and climate. First, by incorporating Zipf's law, URBANMOD-ZIPF substantially improves the accuracy, and thus reliability, of the global urban land change forecasts (see validations in SI session 1.4 and supplementary table 3 is available online at stacks.iop.org/ERL/14/114037/mmedia). Second, by improving the projections of urban cluster sizes on a log scale (see SI supplementary figures 3 and 4), URBANMOD-ZIPF establishes the previously neglected connection between urban size distribution and the UHI effect, which increases with log urban size (Zhou *et al* 2013, Tan and Li 2015, Li *et al* 2017).

UHI intensification forecasts

We build a two-phase statistical model to project the UHI intensifications resulting from urban land expansion. In the first phase, we project future surface UHI (measured as land surface temperature, LST) and in the second phase, link the resulting LST to air temperature (AT). In the first phase, we use sigmoid transformation and multiple regression to model the nonlinear relationship between urban cluster size and surface UHI (Zhou *et al* 2013), measured with the spatially continuous observations of LST from National Aeronautics and Space Administration's Moderate Resolution Imaging Spectroradiometer. Although both linear (Tan and Li 2015, Li *et al* 2017) and sigmoid-based nonlinear (Zhou *et al* 2013) UHI-urban-size relationships have been reported in previous regional studies, our statistical tests at the global scale show that the sigmoid function outperforms the linear one (see SI session 2.2 and supplementary table 5). Separate regressions are run for surface UHIs during daytime and nighttime, in summer and winter, in different climate regions, and for four quantiles of LSTs within urban clusters. In our analyses, summer includes June, July, August and winter includes December, January, February in the Northern Hemisphere; these two seasons include the opposite months

(DJF in summer, JJA in winter) in the Southern Hemisphere.

These regressions are then used to forecast surface UHI intensifications resulting from increases in urban cluster sizes and conversion to urban lands. In the second phase, we model the relationship between LST and the daily maximum and minimum air temperature (Kloog *et al* 2014), with observations from the Global Historical Climatology Network-Daily version-3 dataset (Menne *et al* 2012). This relationship is then applied to forecast increases in air temperature resulting from surface UHI intensification. The ranges of coefficients in these two models are used in a multiplication error propagation formula to assess the uncertainties in the resulting UHI projections. The UHI models are built separately for different Köppen–Geiger climate zones: arid, tropical, temperate and cold climates (Kottek *et al* 2006). Arid zones are where annual precipitation is less than 65% of the potential evapotranspiration. The rest of the world is divided into tropical, temperate or cold zones according to the average temperature of the coldest month: higher than 18 °C as tropical; −3 °C–18 °C as temperate; and lower than −3 °C as cold regions. Although precipitation is not considered in distinguishing the latter three zones, the tropical is usually more humid than the temperate, which is wetter than the cold zones. See supporting information for more details on the urban expansion and UHI models.

Population exposure to warming induced by urban expansion- and GHG emission

To estimate population exposure, we first calculate urban population densities by calculating the reciprocals of the region-specific urban land per capita and then multiply them with the spatially explicit forecasts of warming induced by urban expansion and GHG emission. The latter is represented by the ensemble average of downscaled CMIP5 multi-model simulations under a medium emission scenario—the Representative Concentration Pathway (RCP) 4.5. By comparing with the ensemble average of a medium scenario, we aim to contextualize the importance of urban expansion-warming, acknowledging that the ranges of uncertainties will be larger if multiple models and scenarios are considered. Here we only quantify the uncertainties of urban expansion-warming because those of GHG emission-warming are not the focus of this work.

The downscaled CMIP5 simulation products used here is the NASA Earth Exchange Global Daily Downscaled Projections (NEX-GDDP) dataset (Thrasher *et al* 2012). NEX-GDDP downscales the CMIP5 ensemble outputs into 0.25° by 0.25° resolution, which is the highest spatial resolution available for assessing GHG-induced warming at local to regional scales. Admittedly, calculating the ratio of urban expansion- and GHG emissions-warming separately overlooks the physical interactions between these two processes. According to previous studies using regional climate models (RCMs), the interactive effects between urban expansion and GHG emissions mainly reduces nighttime warming by 0.5 °C (by 2100) (Krayenhoff *et al* 2018) or less (by 2050) (Yang *et al* 2016). Neglecting such interaction is a necessary compromise in order to estimate urban expansion-induced warming at the global scale, since even the finest resolution supported by existing global-scale general circulation models (GCMs; such as the 0.23° by 0.31° in the Community Earth System Model (Hurrell *et al* 2013)) is not enough to resolve the climatic effects of urban expansion.

One caveat worth noting is that the warming exposure estimated here only include the outdoor temperature, rather than the actual climate conditions directly experienced by future urban population. Since urban residents spend the majority of their time indoor, exposure to warming also depends on travel patterns, housing conditions, and availability of indoor climate control. Although other factors affecting population exposure to warming are beyond the scope of this analysis, the outdoor climate conditions projected here will have broad implications for the underlying urban infrastructures, which will be discussed below.

Results

Urban land expansion

Globally, according to our forecasts, about 0.6–1.3 million km^2 of land will be converted to urban areas by 2050, representing increases of 78%–171% over 2015 estimates (range depends on different scenarios). More than two-thirds of this urban expansion will occur in Asia (46%–49%) and Africa (16%–25%), which is not surprising given that the majority of urban population growth will be concentrated in these two continents (figure 1). Within Asia, the bulk of this land expansion will occur in China (19%–22%) rather than India (9%–12%), although India's urban population will grow faster. Low-income sub-Saharan Africa will concentrate 13%–23% of all urban expansion worldwide. Magnitudes of urban expansion vary substantially across different scenarios, mainly driven by different rates of urbanization and economic growth (figure 2(a)). The SSPs represent ranges of socioeconomic challenges for climate mitigation (low in SSP1 and SSP4; intermediate in SSP2; high in SSP3 and SSP5) and adaptations (low in SSP1 and SSP5; intermediate in SSP2; high in SSP3 and SSP4) (O'Neill *et al* 2015). It is worth noting that the second largest amount of urban expansion will occur in the sustainability (SSP1) scenario, where both mitigation and adaptation challenges are small; while the least expansion will occur in the regional rivalry (SSP3) scenario, where both challenges are big.

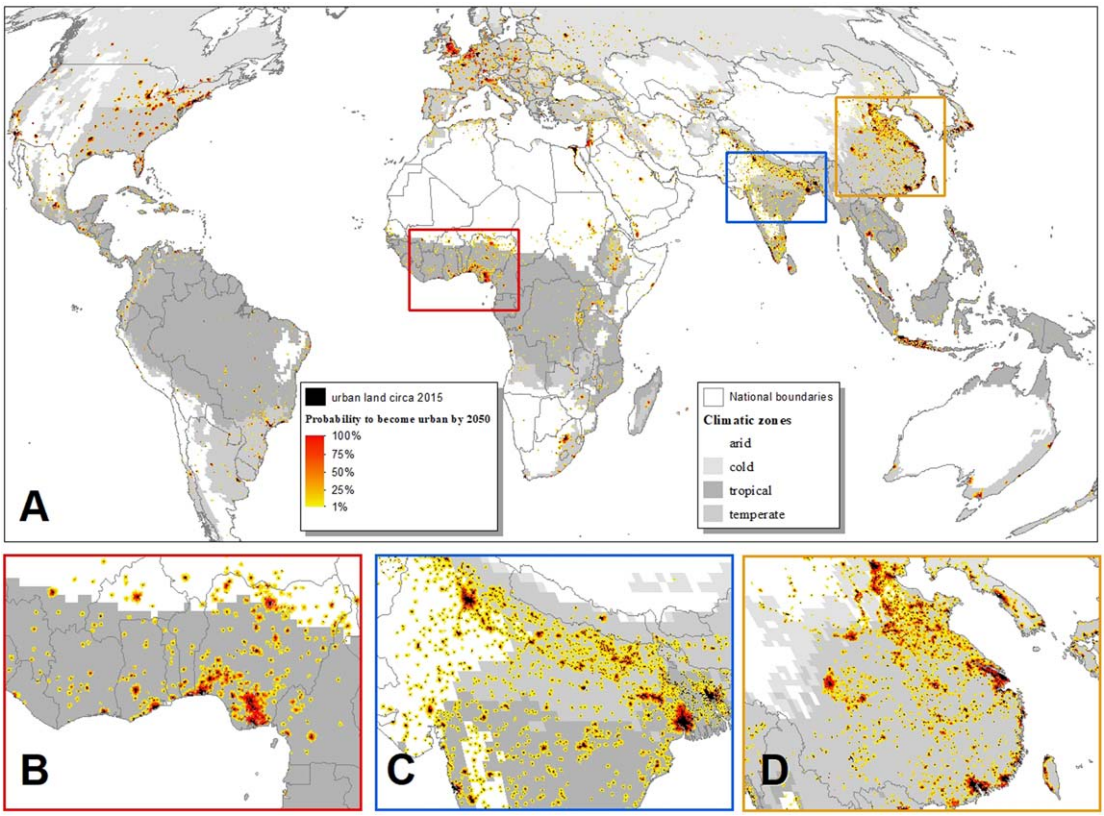

Figure 1. Global forecasts of probabilities of urban expansion through 2050, under the SSP5 scenario.

Despite variations among scenarios, they share similar portions of urban expansion across different climate zones. Our results show that more than 70% of the new urban lands will concentrate in the more humid temperate and tropical zones, while less will occur in the dryer cold and arid zones (figure 2(a)). In developed regions, such as North America and Europe, urban expansion will continue to take place in temperate and cold zones. In China, most of the expansion will occur in temperate zones, the eastern and southern parts of the country; while in India, about half will occur in the temperate/arid north and the rest in the tropical south. In other rapidly developing regions, such as Latin America, Southeast Asia, and Sub-Saharan Africa, the majority of new urban lands will be located in tropical zones (figure 1). These geographic variations suggest that future urban areas in warmer tropical/arid zones tend to be less developed and affluent compared to their counterparts in the colder climates, which is a continuation of historical trends.

UHI intensification

Our results show that urban land expansion through 2050 will lead to warming of surface air temperature (hereafter referred to as 'urban expansion-warming'), which is about 40%–70% as strong as that caused by GHG emissions (hereafter referred to as 'GHG emissions-warming'; figure 2 and table 1). During summer, urban expansion will increase daily minimum and maximum temperatures by 0.5°C–0.7 °C on average (up to ~3 °C in some locations), which is about 39%–64% (up to >200%) as strong as the GHG emissions-induced warming (multi-model ensemble average in the IPCC RCP 4.5 scenario). During winter, the urban expansion-warming will be weaker: on average 0.4 °C–0.6 °C (up to ~2 °C), about 43%–65% (up to ~170%) as strong as the GHG emissions-warming. Despite varying magnitudes of urban expansion, intensities of the subsequent warming are relatively similar across scenarios (table 1). Since UHI depends on the sigmoid function of log urban cluster sizes, the warming saturates in scenarios with more urban expansion. These results of similar warming across scenarios suggest that urban expansion-warming will remain a concern regarding extreme heat risks, even if the pathway with the lowest challenges from emissions-warming (SSP1) is taken.

Urban expansion-induced warming varies significantly across and within climatic zones (figure 2). As scenarios of various urban structures (Güneralp *et al* 2017) are not considered here, the existing fractions of green space, building geometry, construction materials, and energy infrastructures are assumed to be continued in future urban expansion. The expansion-warming is the strongest (on average 0.8 °C–1 °C) and most varied (up to >2 °C) in temperate and cold climates, where GHG-induced warming is also strong but less varied. Urban areas in the tropical and

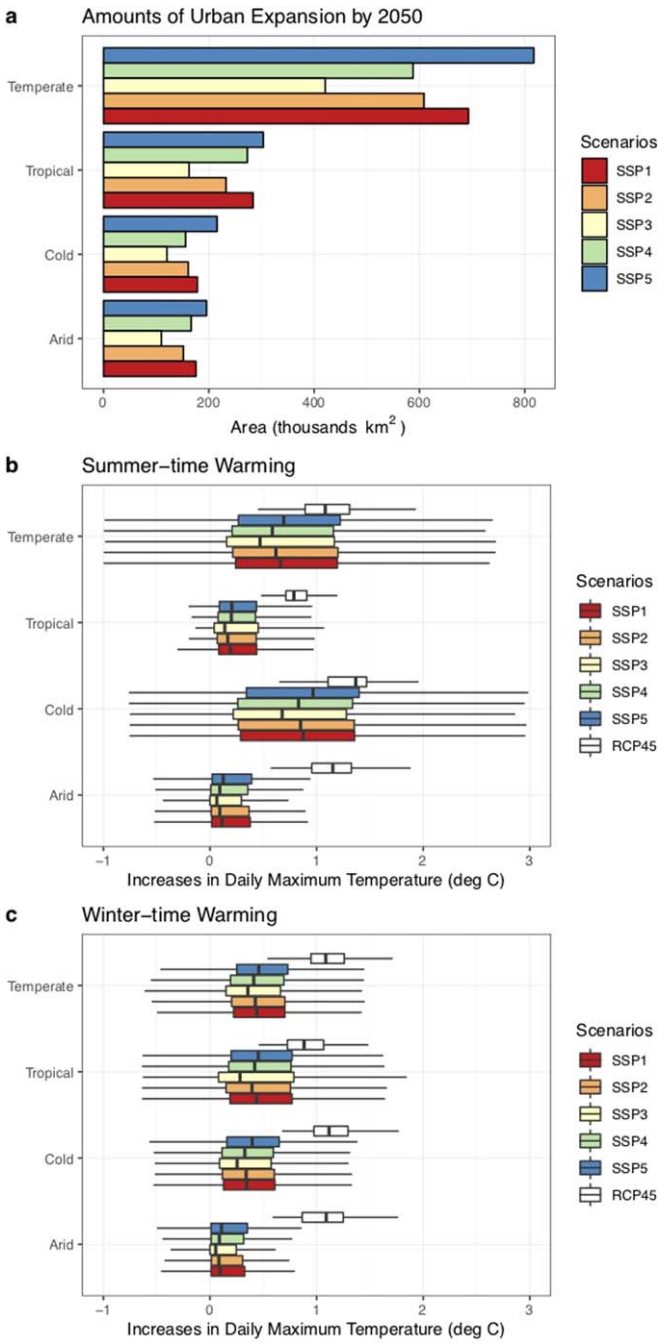

Figure 2. Amounts of forecasted urban expansion across five SSP scenarios by 2050 in different climate zones (a). Probability-weighted boxplots of the increases in daily maximum air temperature in summer (b) and winter (c) due to urban expansion (colored; SSPs) and GHG emissions (white; RCP45). The boxes represent 25%–75% quantiles and the whiskers represent 5%–95% quantiles.

arid climates will experience weaker but still substantial expansion-warming: on average 0.2 °C–0.3 °C, up to >1 °C. Urban expansion-warming in the tropical zone is relatively more important because GHG emissions-warming there is weaker compared to other zones. Urban expansion-warming in the arid zone is weaker on average due to stronger evapotranspiration from urban green spaces compared to the less vegetated adjacent rural lands, which is consistent with the literature on urban cool islands in arid climates (Haashemi *et al* 2016). Combined with the magnitudes of urban expansion, our results highlight temperate and tropical climates. In temperate urban areas, both the magnitude of expansion and the subsequent warming are the most prominent, whereas the tropical regions experience the weakest emissions-warming but considerable urban land expansion and urban expansion-warming.

Within climate zones, warming varies largely across urban clusters of different sizes. Urban clusters of medium sizes, which are 100–5000 km^2 in area, will experience stronger warming with larger variations within the cluster (figure 3). In summer, the hottest cores of medium-sized urban clusters will increase in

Table 1. Probability-weighted mean urban expansion-warming (°C) in different seasons, time of day, climate zones, and SSP scenarios. The numbers in the parentheses are the significance of this warming relative to GHG-induced warming under the RCP 4.5 scenario. The uncertainty range (±) shows one standard deviation.

			Scenario				
Season	Time of day	Climate	SSP1	SSP2	SSP3	SSP4	SSP5
Summer	Daytime	Arid	0.19 ± 0.03 (17% ± 3%)	0.18 ± 0.03 (16% ± 2%)	0.16 ± 0.02 (13% ± 2%)	0.17 ± 0.03 (15% ± 2%)	0.20 ± 0.03 (18% ± 3%)
		Cold	0.96 ± 0.17 (74% ± 13%)	0.94 ± 0.17 (72% ± 13%)	0.85 ± 0.15 (65% ± 12%)	0.93 ± 0.16 (71% ± 13%)	1.03 ± 0.18 (79% ± 14%)
		Tropical	0.30 ± 0.08 (36% ± 10%)	0.28 ± 0.08 (35% ± 10%)	0.27 ± 0.08 (33% ± 9%)	0.29 ± 0.08 (35% ± 10%)	0.30 ± 0.08 (37% ± 10%)
		Temperate	0.70 ± 0.09 (64% ± 8%)	0.68 ± 0.09 (62% ± 8%)	0.62 ± 0.08 (56% ± 7%)	0.66 ± 0.09 (60% ± 8%)	0.74 ± 0.09 (67% ± 9%)
		All	0.57 ± 0.09 (52% ± 8%)	0.56 ± 0.09 (51% ± 8%)	0.50 ± 0.08 (46% ± 7%)	0.53 ± 0.08 (49% ± 8%)	0.61 ± 0.10 (55% ± 9%)
	Nighttime	Arid	0.52 ± 0.08 (50% ± 8%)	0.52 ± 0.08 (49% ± 7%)	0.47 ± 0.07 (44% ± 7%)	0.51 ± 0.08 (49% ± 7%)	0.55 ± 0.08 (53% ± 8%)
		Cold	0.85 ± 0.25 (78% ± 23%)	0.84 ± 0.25 (76% ± 22%)	0.77 ± 0.22 (70% ± 15%)	0.82 ± 0.24 (75% ± 22%)	0.90 ± 0.26 (82% ± 24%)
		Tropical	0.18 ± 0.02 (23% ± 3%)	0.18 ± 0.02 (22% ± 2%)	0.17 ± 0.02 (21% ± 2%)	0.18 ± 0.02 (22% ± 2%)	0.19 ± 0.02 (24% ± 2%)
		Temperate	0.77 ± 16 (79% ± 17%)	0.77 ± 0.16 (77% ± 16%)	0.70 ± 0.15 (70% ± 15%)	0.75 ± 0.16 (75% ± 16%)	0.83 ± 0.17 (83% ± 17%)
		All	0.62 ± 0.13 (62% ± 13%)	0.61 ± 0.13 (61% ± 13%)	0.56 ± 0.12 (55% ± 11%)	0.59 ± 0.12 (58% ± 12%)	0.66 ± 0.12 (66% ± 14%)
Winter	Daytime	Arid	0.19 ± 0.03 (18% ± 3%)	0.18 ± 0.03 (17% ± 2%)	0.15 ± 0.02 (14% ± 2%)	0.18 ± 0.03 (17% ± 2%)	0.20 ± 0.03 (19% ± 3%)
		Cold	0.40 ± 0.11 (40% ± 11%)	0.39 ± 0.11 (39% ± 11%)	0.36 ± 0.10 (35% ± 10%)	0.39 ± 0.11 (38% ± 11%)	0.44 ± 0.12 (44% ± 12%)
		Tropical	0.69 ± 0.06 (81% ± 6%)	0.64 ± 0.05 (76% ± 6%)	0.60 ± 0.05 (69% ± 6%)	0.66 ± 0.05 (77% ± 6%)	0.70 ± 0.06 (83% ± 7%)
		Temperate	0.58 ± 0.06 (58% ± 6%)	0.57 ± 0.06 (57% ± 6%)	0.51 ± 0.05 (52% ± 5%)	0.56 ± 0.06 (56% ± 6%)	0.60 ± 0.06 (61% ± 6%)
		All	0.53 ± 0.06 (55% ± 6%)	0.51 ± 0.06 (53% ± 6%)	0.46 ± 0.05 (48% ± 5%)	0.51 ± 0.06 (53% ± 6%)	0.55 ± 0.06 (58% ± 7%)
	Nighttime	Arid	0.66 (70%)	0.65 (69%)	0.58 (64%)	0.66 (71%)	0.68 (72%)
		Cold	0.71 (54%)	0.68 (52%)	0.63 (47%)	0.68 (51%)	0.74 (56%)
		Tropical	0.55 (68%)	0.52 (64%)	0.48 (61%)	0.53 (65%)	0.56 (70%)
		Temperate	0.40 (42%)	0.39 (41%)	0.36 (39%)	0.39 (40%)	0.41 (43%)
		All	0.53 ± 0.07 (56% ± 7%)	0.51 ± 0.06 (54% ± 7%)	0.47 ± 0.06 (51% ± 6%)	0.52 ± 0.06 (54% ± 7%)	0.54 ± 0.07 (57% ± 7%)

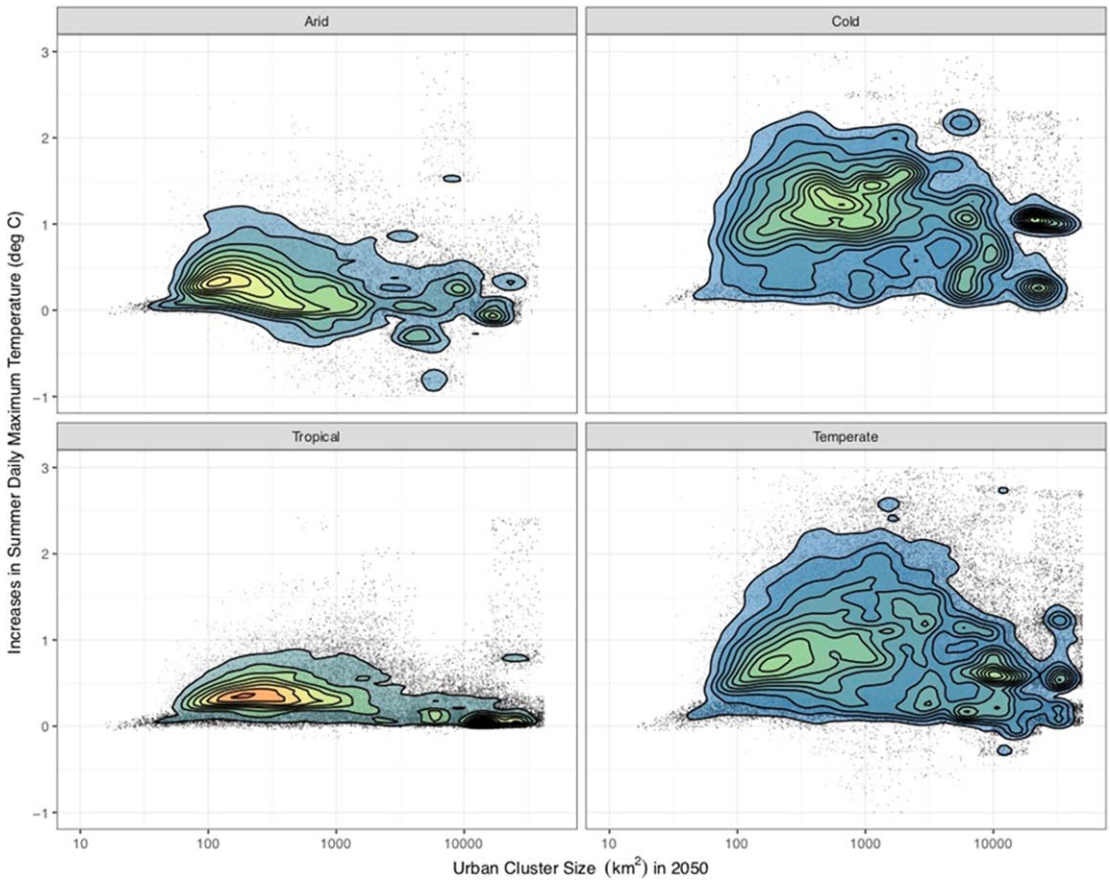

Figure 3. Urban expansion-induced increases in summer daily maximum air temperature and the sizes of urban clusters in 2050. Every 5 by 5 km geographic grid is plotted as a black dot, whose *x*-axis coordinate is the size of the cluster it is located in and transparency is the probability of becoming urban land. A kernel density plot is superimposed on the scatterplot, with colors from blue to red representing increasing point density. Four subplots correspond to arid, cold, tropical and temperate climates.

daily maximum temperatures by up to 2 °C–3 °C in temperate/cold climates and by up to 1 °C in arid/tropical climates. These medium-sized urban clusters warm more intensively because the UHI as a sigmoid function of logarithmic size has the steepest slope at around 100 km^2 and starts to plateau beyond 5000 km^2 (supplementary figure 5). Such urban clusters, usually administered as medium-sized municipalities, may lack sufficient capacity to adapt to the stronger warming compared to the larger cities (Shi *et al* 2016).

Exposures to heat risk

By overlaying our forecasts with socioeconomic data, we identify the urban areas that are exposed to greater heat risks than previously assumed if urban expansion-warming was not considered. Without considering the additional warming forecasted here, the regions with the most heat risk-exposures are those exposed to both stronger GHG emissions-warming and the lack of financial and governance capacities to adapt (O'Brien and Leichenko 2000). We build on and expand this framework by contrasting the ratios of urban expansion- to GHG emissions-induced warmings versus the capacities for climate adaptation, approximated by GDP per capita due to the lack of governance indicators in future scenarios (figure 4). This new geographic pattern of heat-risk-exposure can only be revealed by the global scale forecasts of urban land expansion and heat island intensification.

Overall, the ratio of expansion-warming is positively associated with adaptation capacity, because urban expansion and the subsequent warming are usually concurrent with economic growth. Divided by the global average GDP per capita, the right side of figure 4 shows the more affluent regions where expansion-warming will be 50%–120% of emissions-warming. Most urban areas in these regions are located in the cold and temperate climates, which have been shown to be more suitable for economic development (Nordhaus 2006). Given the largest magnitude of urban expansion and the strongest expansion-warming in temperate zones, these regions need to effectively implement adaptations in a large swath of urban areas. The larger variation of expansion-warming in temperate zones (figure 3) suggests the possibility to prioritize adaptations in urban areas that will experience more severe warming.

The left side of figure 4 shows the regions with lower GDP per capita and substantial GHG emissions-induced warming, most of which are located in arid

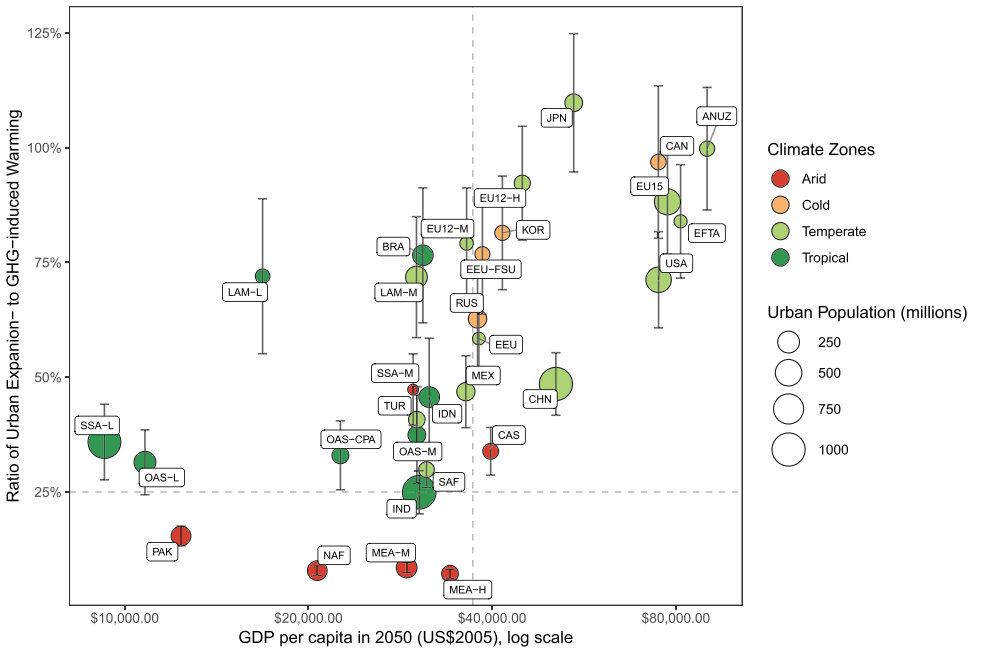

Figure 4. Region-averaged Ratio of urban expansion-induced (SSP5) to GHG emissions-induced (RCP4.5) warming versus the GDP per capita in 2050. Each region or country is represented by a circle, whose size is proportional to the urban population and whose color represents the climatic zone where the majority of the urban areas are located. The horizontal dashed line represents urban expansion-warming is at least 25% as significant as emissions-warming; the vertical dashed line is the global average GDP per capita. Error bars show one standard deviation. (Detailed regions definition in supplementary table 1. -L: low-income; -M: medium income; -H: high-income; ANUZ: Australia, New Zealand; CAN: Canada; EEU: Eastern Europe; EFTA: Iceland, Norway, Switzerland; EU: European Union; JPN: Japan; TUR: Turkey; USA: United States of America; CAS: Central Asia; RUS: Russia; CHN: China; IDN: Indonesia; IND: India; KOR: South Korea; OAS: Other Asia; MEA: Middle East Asia; NAF: North Africa; PAK: Pakistan, Afghanistan; SAF: South Africa; SSA: Sub-Saharan Africa; BRA: Brazil; LAM: Latin America; MEX: Mexico.)

and tropical climates. By contrasting expansion- and emissions-warming, our work divides these regions into two quadrants. Regions in the upper-left quadrant, mostly in the tropical/temperate Global South, are the most heat-risk-prone regions with low economic capacities but substantial warming caused by urban land expansion. Albeit some are located in the temperate zones; the majority of these risk-prone urban areas will be in the tropical zones. Regions in the low-left quadrant, mostly in the arid Africa/Middle-East, will experience weaker expansion-warming on average due to the cooling effects in some urban areas (figure 3). Despite the weaker average, the hotter parts of arid urban clusters will still experience expansion-warming comparable to their tropical counterparts. Besides from less adaptive capacities, knowledge for risk reduction in these regions is also sparser or less well-documented in academic literature: for instance, a meta-analysis (Romero-Lankao *et al* 2012) found that the majority of temperature-related urban vulnerability studies in existing literature were conducted in the temperate/cold, rather than the tropical/arid, zones. In the latter zones, we have relatively less understanding of what factors contribute more to higher urban vulnerability to heat risks. Within these regions, urban areas belonging to medium-sized urban clusters, in particular, will be exposed to greater heat risks, due to the more intense urban expansion-warming. These regions will face the challenge of first filling the knowledge gap in heat-related urban vulnerability and then upscaling the knowledge-based adaptations to considerable amounts of new urban areas. In total, about half of the world's urban population will live in the most risk-prone regions in the upper-left quadrant of figure 4 by 2050.

Discussions

Land and climate dimensions of urbanization

The World Urbanization Prospects (WUP) and IPCC reports released by the United Nations (UN) have been the primary sources of global urbanization and climate change projections. However, the WUP urbanization projections only show country-level urban population growth, missing intra-country distributions and the changes in urban land cover (UN DESA 2014); the IPCC projections, although acknowledging the importance of UHI, do not include the local climate effects of future urbanization (Revi *et al* 2014). Improving upon the shorter-term urban expansion forecasts to 2030 (Seto *et al* 2012), our study complements the UN urbanization and climate projections by developing spatially explicit, probabilistic forecasts of global urban land expansion and heat island intensification through 2050. Our analysis reveals the spatial patterns of land and climate consequences of demographic urbanization. For instance, although it is well known that urban population will grow rapidly in Asia and Africa (UN

DESA 2014), our results further show that, if our assumptions on urban size distribute hold in the future, the majority of the urban expansion there will occur in the temperate and tropical zones, concentrating more around medium- to large-sized urban clusters (figure 1, supplementary figure 3). Given that expansion-warming is substantial in temperate/tropical zones (figures 2(b) and (c)) and is stronger in medium-sized urban clusters (figure 3), the land and climate dimensions present in our analysis reveal that the urban population in South/Southeast Asian and Sub-Saharan African countries will be exposed to greater heat risks than previously assumed (figure 4).

Our forecasts assume the dependence of urban expansion on economic and demographic growth, and on the current spatial- and size-distributions of urban clusters, all of which include inevitable uncertainties. The SSP scenarios used here have incorporated some uncertainties in economic and population growth by including several plausible development pathways with different levels of challenges in mitigating and adapting to emissions-warming (O'Neill *et al* 2015). Despite these uncertain challenges, our results show consistently substantial magnitudes of urban expansion and expansion-warming across SSPs, especially in the sustainability (SSP1) scenario (figure 2). Our analysis suggests that even if the sustainable pathway, regarding emissions-warming, is taken, the climatic and environmental impacts from urbanization will remain substantial. Additionally, another important, but not included, aspect of demographic change can also influence the magnitudes of urban expansion: household size. Given a fixed population size, larger amounts of smaller households result in higher per capita consumption, often manifested as urban sprawl and more expansion (Liu *et al* 2003). The average household sizes are currently >4 in most of the risk-prone regions identified here, compared to ~2 in other parts of the world (UN DESA 2017). If the worldwide trends of declining household sizes also occur in the risk-prone regions, the magnitudes of future urban expansion and expansion-warming will be substantially larger than forecasted, further jeopardizing the at-risk population.

Our analysis assumes the continuation of current spatial- and size-distributions of urban clusters, but they can be altered by policy interventions. In China, for instance, the registration system limits the population growth of the country's megacities in temperate/cold zones, pushing expansion to smaller cities; while the Western Development Program accelerates expansion in western Chinese cities, most of which are in arid/cold zones (Chang and Brada 2006, Deng and Bai 2014). In the United States, policies like relatively lower taxation on fuels and more subsidies for highway encourage automobile over public transit use, leading to urban sprawl and thus larger urban clusters (Teaford 2007); local policies restricting urban development in the arid west coast and cold northeast have pushed some urban expansion to the temperate/tropical southern states where zoning regulations are weaker (Glaeser and Kahn 2010). The decision to limit or encourage urban expansion should depend on whether the municipalities can effectively handle the consequences of expansion, such as loss of farmland (d'Amour *et al* 2017) and habitat (Seto *et al* 2012), increase in resource consumption (Liu *et al* 2003, Broto *et al* 2012), and warming of regional climate (Georgescu *et al* 2014). Regarding regional climate, our analysis (figure 3) provide complementary information for decision-making by showing the variations in expansion-warming across urban cluster sizes and climate zones, which have differentiated impacts on human health, energy system, and urban infrastructures.

The impacts of warming tend to be negative during summer but positive during winter. Unlike the more seasonally uniform GHG emissions-warming, our results show stronger urban expansion-warming in the summer than in the winter (figure 2; table 1), suggesting that the overall annual impacts may be negative. The specific local impacts of warming, however, depend on the adaptive capacity and the severity of emissions- and expansion-warming, all of which vary geographically. Our spatially explicit forecasts of urban expansion and subsequent warming provide the bases to discuss how urbanization will reshape the differentiated warming impacts across the world.

Implications for human health

In the coming decades, GHG emissions-warming alone will increase the temperature-related mortality rates by 3%–13% in tropical zones but will reduce those by <1% in temperate/cold zones (Gasparrini *et al* 2017). According to the observed U-shape temperature-mortality relationship (Gasparrini *et al* 2015), the overall warming will increase mortality risk in summer and lower mortality risk in winter. The actual balance will vary by many factors including the location of the city. The U-shape curve differs dramatically by city. The urban expansion-warming forecasted here is likely to exacerbate the heat-related health risks in two ways. First, in temperate/cold zones, since summer-time expansion-warming will be stronger than winter-time expansion-warming (figure 2), the negative impacts are likely to exceed the positive ones, leading to net increases in mortality rates. Second, in tropical zones, the already severe negative impacts from emissions-warming will be further compounded by the additional expansion-warming and the lack of adaptive capacity (figure 4).

The large amounts of urban expansion and the substantial expansion-warming in wetter tropical/temperate zones will coincide with the heat stress from rising humidity. The apparent temperature (AP) (Sherwood and Huber 2010, Li *et al* 2018), measured with a heat stress index using both temperature and humidity, can account for the full physiological

impacts of heat on human bodies. GHG emissions is projected to increase AP faster than air temperature by 0.06 °C per decade (under RCP4.5) globally, which will be three times faster in the wetter regions due to rapidly rising humidity (Li *et al* 2018). The geographic distribution of faster-rising AP largely overlaps with the most risk-prone regions identified here (figure 4) with considerable expansion-warming and less adaptive capacity: Latin America, Sub-Saharan Africa, South and Southeast Asia. However, the net effect on AP from urban expansion is still uncertain because it also reduces humidity locally by removing vegetation (Adebayo 1991, Kaiser *et al* 2016). Compared to installing green roofs (Klein and Coffman 2015), urban adaptations that can reduce temperature without increasing humidity, such as albedo enhancement (Georgescu *et al* 2014) or preserving green space (Doick *et al* 2014), deserve more consideration particularly in the tropical/temperate zones, where more than two-thirds of future urban expansion will occur (figure 2).

Implications for energy consumption

One of the most effective measures to reduce heat-related mortalities—installing indoor cooling—can significantly increase energy demand and requires sufficient financial resources. Rapid economic development will make air conditioning (AC) more affordable in the future medium- to high-income countries, reducing the health risks albeit at the cost of soaring energy consumption. For instance, by mid-century, due to rising income and growing population, cooling energy demand in India and China will rise to >30 EJ and >40 EJ respectively, which will be further raised by a third due to emissions-warming (Isaac and van Vuuren 2009). Extra cooling energy demand in these countries from urban expansion can rise to the magnitude of ten EJ since the majority of their urban expansion will occur in the temperate/tropical zones, where summer-time expansion-warming is 30%–70% as strong as the emissions-warming (table 1; figure 2). There is also a positive feedback between expansion-warming and widely-adopted AC systems, because the latter release waste heat which enhances UHI which further increases cooling energy use (Salamanca *et al* 2014). Among the most heat-risk-prone regions identified in this study, AC installation rates will remain low in the low-income Latin American, Southeast Asian, and Sub-Saharan African countries by 2050. Due to insufficient financial resources, less than half of the households in these countries can afford AC, leaving them especially susceptible to heat-related health risks (SI 2.5 and supplementary figure 1).

Winter-time warming can result in energy savings by reducing heating requirements in the temperate/cold zones. However, our results suggest that the energy savings on heating are not likely to outweigh the extra costs on cooling. In the temperate zones, expansion-warming in summer will be ~60% stronger than that in the winter; in the cold zones, the former is as twice as strong as the latter (table 1). Savings on heating energy in the winter in the temperate zones may be further reduced by the warming adaptation discussed above, such as installing cool roofs. That is because the cooling effects of high-reflectance-materials persist in the winter, diminishing the energy savings.

Implications for grey and green infrastructures

In addition to the energy system, warming can also negatively impact grey and green infrastructures, since both have suitable temperature ranges to function effectively. One example of potential grey infrastructure damage is the pavement degradation of roads, which tends to accelerate when the temperature rises beyond the suitable range of the selected pavement material. Because stationary future climate was often assumed when selecting materials, emissions-warming alone has been shown to severely accelerate pavement degradation in the United States and Europe by mid-century, costing extra tens of billions US$ (Underwood *et al* 2017, Forzieri *et al* 2018). In these regions, costs from pavement degradation will rise even higher considering the expansion-warming forecasted there will be >70% as strong as the emissions-warming (figure 4). Although most of the risk-prone regions identified here will experience relatively weaker expansion-warming, the extra costs will be more burdensome because their GDP per capita will be less than half of the US's (figure 4). Given that most infrastructures in the risk-prone regions are yet to be built, future degradation of grey infrastructures could be mitigated, if the material selection considers both emissions- and expansion-warming.

Urban green infrastructure has received increasing attention because of its potential to reduce climate change impacts, such as the intensifying heatwaves and floods (Gill *et al* 2007). There is evidence suggesting that, in the past, the UHI effect actually enhances green infrastructures, by extending the growing season in cold regions (Zhao *et al* 2016). However, it is unclear whether future urban expansion-warm will continue to benefit green infrastructure because the combined emissions- and expansion-warming may push urban vegetation out of the suitable temperature ranges during hot days, impairing their health. Moreover, the UHI effect has been shown to increase the water demand for irrigation (Guhathakurta and Gober 2007), which may not be met as urbanization and climate change were projected to cause water shortage for an additional ~1 billion urban dwellers by 2050 (McDonald *et al* 2011). In the more water-scarce arid zones, if the irrigation demand is unmet, the urban cooling effects will be nullified, leaving the expansion-warming similar to that in the tropical zones (left

column of figure 3). In this case, regions in the lower-left quadrant of figure 4 will shift to the upper-left, increasing risk-prone urban populations by hundreds of millions. Similar to their grey counterparts, the to-be-built green infrastructures in these risk-prone regions also provide enormous opportunities. Seizing these opportunities requires selecting the appropriate heat- and drought-tolerant plant communities and preserving sufficiently large urban green spaces to better harness their benefits.

Conclusion

Using models capable of capturing log-scale urban size distribution and log-size dependent UHIs, we develop global spatially-explicit forecasts of urban land expansion and heat island intensification through 2050. Our analysis shows that urban expansion will cause warming as significant as, at places even stronger than, that caused by GHG emissions. Combined with the spatially varying emissions-warming and socioeconomic development, our work reveals a new global geography of the increasing extreme heat risks. This previously unexamined extra warming will expose billions of urban dwellers, primarily in the tropical Global South, to greater extreme heat risks. This enormous urban land expansion and the subsequent warming are likely to occur in a relatively short time window of three decades. Policy interventions to restrict or redistribute urban expansion or planning strategies to mitigate urban heat, as discussed above, are needed particularly in the vulnerable urban areas identified, in order to reduce the wide ranges of impacts on human health, energy systems, urban ecosystems, and infrastructures.

Data that support the findings of this study have been deposited on https://urban.yale.edu, through figshare:

Urban land expansion: https://figshare.com/s/48ae29774f778ccb6ac3;

Urban heat island intensification: https://figshare.com/s/d696842e80e8b02e9c7a.

Acknowledgments

This research was supported by the NASA Earth and Space Science Fellowship (NESSF) Program (grant 80NSSC17K0447), the Yale Institute of Biospheric Studies, the Yale Hixon Center for Urban Ecology, the Yale Tropical Resources Institute, and a Yale University Graduate Fellowship. KCS acknowledges the support of NASA Land Cover/Land Use Change (LCLUC) Program (grant NNX17AH98G). X Li and X Liu acknowledge the support of the National Key R & D Program of China (grant 2017YFA0604402 and 2017YFA0604404). The model runs were supported by the Yale University Center Research Computing's High Performance Cluster.

Author contributions

KH and KCS designed the research. KH performed research. X Li and X Liu contributed ideas to the research. KH and KCS wrote the paper.

ORCID iDs

Kangning Huang https://orcid.org/0000-0001-6877-9442

References

Adebayo Y R 1991 Day-time effects of urbanization on relative humidity and vapour pressure in a tropical city *Theor. Appl. Climatol.* **43** 17–30

Broto V C, Allen A and Rapoport E 2012 Interdisciplinary perspectives on urban metabolism *J. Ind. Ecol.* **16** 851–61

Chang G H and Brada J C 2006 The paradox of China's growing under-urbanization *Econ. Syst.* **30** 24–40

Chen L and Frauenfeld O W 2016 Impacts of urbanization on future climate in China *Clim. Dyn.* **47** 345–57

Cristelli M, Batty M and Pietronero L 2012 There is more than a power law in Zipf *Sci. Rep.* **2** 812

d'Amour C B, Reitsma F, Baiocchi G, Barthel S, Güneralp B, Erb K-H, Haberl H, Creutzig F and Seto K C 2017 Future urban land expansion and implications for global croplands *Proc. Natl Acad. Sci.* **114** 8939–44

Deng X and Bai X 2014 Sustainable urbanization in western China *Environ. Sci. Policy Sustain. Dev.* **56** 12–24

Doick K J, Peace A and Hutchings T R 2014 The role of one large greenspace in mitigating London's nocturnal urban heat island *Sci. Total Environ.* **493** 662–71

Forzieri G, Bianchi A, Silva F B E, Marin Herrera M A, Leblois A, Lavalle C, Aerts J C J H and Feyen L 2018 Escalating impacts of climate extremes on critical infrastructures in Europe *Glob. Environ. Change* **48** 97–107

Fragkias M and Seto K 2009 Evolving rank-size distributions of intra-metropolitan urban clusters in South China *Computers, Environment and Urban Systems* **33** 189–99

Gabaix X 1999 Zipf's law for cities: an explanation *Q. J. Econ.* **114** 739–67

Gasparrini A *et al* 2015 Mortality risk attributable to high and low ambient temperature: a multicountry observational study *Lancet* **386** 369–75

Gasparrini A *et al* 2017 Projections of temperature-related excess mortality under climate change scenarios *Lancet Planet. Health* **1** e360–7

Georgescu M, Morefield P E, Bierwagen B G and Weaver C P 2014 Urban adaptation can roll back warming of emerging megapolitan regions *Proc. Natl Acad. Sci.* **111** 2909–14

Georgescu M, Moustaoui M, Mahalov A and Dudhia J 2013 Summer-time climate impacts of projected megapolitan expansion in Arizona *Nat. Clim. Change* **3** 37–41

Gill S E, Handley J F, Ennos A R and Pauleit S 2007 Adapting cities for climate change: the role of the green infrastructure *Built Environ.* **33** 115–33

Glaeser E L and Kahn M E 2010 The greenness of cities: carbon dioxide emissions and urban development *J. Urban Econ.* **67** 404–18

Guhathakurta S and Gober P 2007 The impact of the phoenix urban heat island on residential water use *J. Am. Plan. Assoc.* **73** 317–29

Güneralp B and Seto K C 2013 Futures of global urban expansion: uncertainties and implications for biodiversity conservation *Environ. Res. Lett.* **8** 014025

Güneralp B, Zhou Y, Ürge-Vorsatz D, Gupta M, Yu S, Patel P L, Fragkias M, Li X and Seto K C 2017 Global scenarios of urban density and its impacts on building energy use through 2050 *Proc. Natl Acad. Sci.* **114** 8945–50

Haashemi S, Weng Q, Darvishi A and Alavipanah S K 2016 Seasonal variations of the surface urban heat Island in a semi-arid city *Remote Sens.* **8** 352

Hurrell J W *et al* 2013 The community earth system model: a framework for collaborative research *Bull. Am. Meteorol. Soc.* **94** 1339–60

Isaac M and van Vuuren D P 2009 Modeling global residential sector energy demand for heating and air conditioning in the context of climate change *Energy Policy* **37** 507–21

Kaiser A, Merckx T and Dyck H V 2016 The Urban Heat Island and its spatial scale dependent impact on survival and development in butterflies of different thermal sensitivity *Ecol. Evol.* **6** 4129–40

Klein P M and Coffman R 2015 Establishment and performance of an experimental green roof under extreme climatic conditions *Sci. Total Environ.* **512–513** 82–93

Kloog I, Nordio F, Coull B A and Schwartz J 2014 Predicting spatiotemporal mean air temperature using MODIS satellite surface temperature measurements across the Northeastern USA *Remote Sens. Environ.* **150** 132–9

Kottek M, Grieser J, Beck C, Rudolf B and Rubel F 2006 World map of the Köppen–Geiger climate classification updated *Meteorol. Z.* **15** 259–63

Krayenhoff E S, Moustaoui M, Broadbent A M, Gupta V and Georgescu M 2018 Diurnal interaction between urban expansion, climate change and adaptation in US cities *Nat. Clim. Change* **8** 1097

Li J, Chen Y D, Gan T Y and Lau N-C 2018 Elevated increases in human-perceived temperature under climate warming *Nat. Clim. Change* **8** 43–7

Li X, Zhou Y, Asrar G R, Imhoff M and Li X 2017 The surface urban heat island response to urban expansion: a panel analysis for the conterminous United States *Sci. Total Environ.* **605–606** 426–35

Liu J, Daily G C, Ehrlich P R and Luck G W 2003 Effects of household dynamics on resource consumption and biodiversity *Nature* **421** 530–3

McDonald R I, Green P, Balk D, Fekete B M, Revenga C, Todd M and Montgomery M 2011 Urban growth, climate change, and freshwater availability *Proc. Natl Acad. Sci.* **108** 6312–7

Menne M J, Durre I, Vose R S, Gleason B E and Houston T G 2012 An overview of the global historical climatology network-daily database *J. Atmos. Ocean. Technol.* **29** 897–910

Merckx T *et al* 2018 Body-size shifts in aquatic and terrestrial urban communities *Nature* **558** 113

Nordhaus W D 2006 Geography and macroeconomics: new data and new findings *Proc. Natl Acad. Sci. USA* **103** 3510–7

O'Brien K L and Leichenko R M 2000 Double exposure: assessing the impacts of climate change within the context of economic globalization *Glob. Environ. Change* **10** 221–32

Oke T R 1982 The energetic basis of the urban heat island *Q. J. R. Meteorol. Soc.* **108** 1–24

O'Neill B C *et al* 2015 The roads ahead: narratives for shared socioeconomic pathways describing world futures in the 21st century *Glob. Environ. Change* **42** 169–180

Pesaresi M *et al* 2013 A global human settlement layer from optical HR/VHR RS data: concept and first results *IEEE J. Sel. Top. Appl. Earth Obs. Remote Sens.* **6** 2102–31

Revi A, Satterthwaite D E, Aragón-Durand F, Corfee-Morlot J, Kiunsi R B R, Pelling M, Roberts D C and Solecki W 2014 Urban areas *Climate Change 2014: Impacts, Adaptation, and Vulnerability. Part A: Global and Sectoral Aspects. Contribution of Working Group II to the Fifth Assessment Report of the Intergovernmental Panel of Climate Change* ed C B Field *et al* (Cambridge: Cambridge University Press) pp 535–612

Riahi K *et al* 2017 The Shared Socioeconomic Pathways and their energy, land use, and greenhouse gas emissions implications: An overview *Global Environmental Change* **42** 153–68

Romero-Lankao P, Qin H and Dickinson K 2012 Urban vulnerability to temperature-related hazards: a meta-analysis and meta-knowledge approach *Glob. Environ. Change* **22** 670–83

Rozenfeld H D, Rybski D, Andrade J S, Batty M, Stanley H E and Makse H A 2008 Laws of population growth *Proc. Natl Acad. Sci.* **105** 18702–7

Salamanca F, Georgescu M, Mahalov A, Moustaoui M and Wang M 2014 Anthropogenic heating of the urban environment due to air conditioning *J. Geophys. Res. Atmos.* **119** 5949–65

Seto K C, Güneralp B and Hutyra L R 2012 Global forecasts of urban expansion to 2030 and direct impacts on biodiversity and carbon pools *Proc. Natl Acad. Sci.* **109** 16083–8

Sherwood S C and Huber M 2010 An adaptability limit to climate change due to heat stress *Proc. Natl Acad. Sci.* **107** 9552–5

Shi L *et al* 2016 Roadmap towards justice in urban climate adaptation research *Nat. Clim. Change Lond.* **6** 131–7

Stone B 2012 *The City and the Coming Climate: Climate Change in the Places We Live* (New York: Cambridge University Press)

Stone B, Vargo J, Liu P, Habeeb D, DeLucia A, Trail M, Hu Y and Russell A 2014 Avoided heat-related mortality through climate adaptation strategies in three US Cities ed I Linkov *PLoS One* **9** e100852

Tan M and Li X 2015 Quantifying the effects of settlement size on urban heat islands in fairly uniform geographic areas *Habitat Int.* **49** 100–6

Teaford J C 2007 *The American Suburb: The Basics* (New York: Routledge)

Thrasher B, Maurer E P, McKellar C and Duffy P B 2012 Technical note: bias correcting climate model simulated daily temperature extremes with quantile mapping *Hydrol. Earth Syst. Sci.* **16** 3309–14

UN DESA 2014 *World Urbanization Prospects: The 2014 Revision, Highlights* (New York: United Nations, Department of Economic and Social Affairs, Population Division)

UN DESA 2017 *Household Size and Composition 2017* (New York: United Nations, Department of Economic and Social Affairs, Population Division) (https://population.un.org/Household)

Underwood B S, Guido Z, Gudipudi P and Feinberg Y 2017 Increased costs to US pavement infrastructure from future temperature rise *Nat. Clim. Change* **7** 704–7

World Bank Group 2019 *World Bank World Development Indicators, 1960-2018* [data collection] *27th Edition* UK Data Service SN: 4814 (http://doi.org/10.5257/wb/wdi/2019-02)

Yang L, Niyogi D, Tewari M, Aliaga D, Chen F, Tian F and Ni G 2016 Contrasting impacts of urban forms on the future thermal environment: example of Beijing metropolitan area *Environ. Res. Lett.* **11** 034018

Zhao S, Liu S and Zhou D 2016 Prevalent vegetation growth enhancement in urban environment *Proc. Natl Acad. Sci.* **113** 6313–8

Zhou B, Rybski D and Kropp J P 2013 On the statistics of urban heat island intensity *Geophys. Res. Lett.* **40** 5486–91